Table IV. Atomic Parameters for Atoms Si and P, and Pseudoatoms Ge′ and P′

	Si	P	Ge′	P′
Slater exponent	1.383	1.600	1.383	1.600
H_{ii} (3s), eV	−17.3	−18.6	−13.25	−16.3
H_{ii} (3p), eV	−9.2	−14.0		

that these really are the electronic reasons behind the stabilities of these structures.

Acknowledgment. This work has been supported by the National Science Foundation under Grant NSF DMR 8019741. We are also grateful to the donors of the Petroleum Research Fund, administered by the American Chemical Society, for their partial support of this research and to the Dreyfus Foundation, who made possible the stay of J.H.B. at Chicago.

Appendix

Both crystal and molecular calculations in this paper used the extended Hückel method.[13] The band structure program was written by M.-H. Whangbo and used in ref 14. We are grateful to Dr. Whangbo for permission to use his program.

Because of the lack of well-established extended Hückel atomic parameters for Ge, we used parameters appropriate for Si, as listed in Table IV. The size of the observed unit cell of GeP was reduced accordingly to produce the nearest-neighbor distances shown in the representative fragment (**4**),

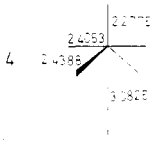

which should be appropriate for Si and P. Each of structures A–D had cell parameters $a = b = 4.8106$ Å and $c = 5.36$ Å. The P and Ge atoms were displaced from their ideal positions in a tetragonally distorted rock salt cell by moving them along c, a distance of $\pm 0.0376c$, the sign at each atom depending on the structure. The two "rock salt" structures considered were R′, a tetragonally distorted NaCl type with this unit cell, and R, an ideal NaCl type with $c = 4.8106$ Å corresponding to a situation in which no Ge–P bonds are broken and each atom has six neighbors at 2.4053 Å. The "TII" structure D′ was obtained from structure D by doubling c and translating one of the layers normal to c by $(a/4, b/4)$ relative to the other.

Energies of each of these structures except D′ were evaluated at the special points[4] $i/8, j/8, k/8$ [$i, j, k = \pm 1$, 3 (8 symmetry-inequivalent points)] and $i/16, j/16, k/16$ [$i, j, k = \pm 1$, 3, 5, or 7 (64 points)]. The Fermi level was computed by assuming each of these points represented an equal volume in the Brillouin zone, and the energy was obtained accordingly. As seen in Table III, the results of these two sets of calculations were essentially identical. In structure D′, only the first set of special points was used.

Molecular calculations were performed on GeP'_5 and PGe'_5 units. In both cases the apical bond distance was 2.2775 Å, and the basal distance was 2.4053 Å when the bond angle was 90°. The molecules were then distorted by increasing θ either with fixed bond distances or by moving the basal atoms parallel to the figure axis, thereby increasing the bond distances slightly, as in the crystals themselves. The average relative energies from this second distortion mode are in Table II. Because the HOMO (filled for 10 electrons per molecule and half-filled for 9) does not change in energy during this distortion, these results are insensitive to the exact electron count at each atomic center. Addition of p orbitals to the ligands does not qualitatively alter these conclusions.

Registry No. GeP, 25324-55-4.

(13) (a) Hoffmann, R. *J. Chem. Phys.* **1963**, *39*, 1397. (b) Hoffmann, R.; Lipscomb, W. N. *Ibid.* **1962**, *36*, 2179; **1962**, *37*, 2872.
(14) Whangbo, M.-H.; Hoffmann, R.; Woodward, R. B. *Proc. R. Soc., London* **1979**, *A366*, 23.

Contribution from the Department of Chemistry, University of Delaware, Newark, Delaware 19711

Electron Distribution and Bonding Patterns in Octahedral Organometallic Complexes of Co(III), Co(I), and Mn(I) with a Ligand Geometry of *fac*-a_3b_2c: A Nuclear Quadrupole Resonance Analysis

T. B. BRILL,* S. J. LANDON, and D. K. TOWLE

Received August 10, 1981

Note is made of the fact that NQR signals of the metal frequently appear in organometallic complexes in which octahedral coordination of the metal occurs with the stoichiometry and structure of *fac*-a_3b_2c. An electrostatic model of the electric field gradient correctly describes the NQR data in $(\eta^5\text{-}C_5H_5)CoI_2c$ and $(\eta^5\text{-}C_5H_5)CoIc_2^+$ complexes (c = CO, $PO_3C_6H_{11}$, $P(OPh)_3$, PPh_3, $AsPh_3$, $SbPh_3$, NC_5H_5, NH_2CH_2Ph (Ph = C_6H_5) and c_2 = ethylenediamine, *o*-phenylenediamine, and bipyridyl). The electrostatic model is most suitable for predominantly σ-donor ligands and works less well for ligands with large π acidity. Comparison of NQR data for Mn(I) complexes of the type $(\eta^5\text{-}C_5H_5)Mn(CO)_2c$ and the above Co(III) complexes indicates the electric field gradient has the opposite sign in these two isoelectronic metals. The inversion is traceable to differences in the 3d orbital electron distribution between Co(III) and Mn(I) which are brought on by the difference in bonding of CO and I. These results help reconcile conflicting discussions that have appeared concerning the electric field gradient of Mn(I) organometallic complexes. The nature of bonding between Co(III) and an uncommon ligand, the phosphonate group, $P(O)(OCH_3)_2$, is revealed to be a weak σ donor with some π-acceptor ability.

Introduction

Compounds of Co(I) and Co(III) having three unique ligands a, b, and c in an octahedral arrangement of stoichiometry *fac*-a_3b_2c are prevalent in organometallic chemistry. There are several reasons why a determination of the ground-state electronic structure of this category of compounds is important.

First, 18e complexes of Co(I) with the formulation Cp-$(Co)b_2$, where b = CO, $P(OR)_3$, and PR_3 (R = alkyl) and Cp = $\eta^5\text{-}C_5H_5$, exhibit strong basic character in the presence of a Lewis acid.[1,2] Similarly, 16e $Cp(Co)b_2$ complexes are Lewis

(1) Cook, D. J.; Davis, J. L.; Kemmitt, R. D. W. *J. Chem. Soc.* **1967**, 1547–1551.

0020-1669/82/1321-1437$01.25/0

acids toward donor ligands. The reaction in both cases is $Cp(Co)b_2 + c \rightarrow Cp(Co)b_2c$, where c is the respective acid or base. The resultant acid–base complexes are 18e species in which cobalt attains approximately octahedral coordination. In terms of the ligands a, b, and c, the geometry of the coordination sphere is *fac*-a_3b_2c. The cyclopentadienyl ring is the a_3 ligand occupying a face of the octahedron. In order to specify the electronic changes at the metal that take place in the acid–base reactions, it is necessary to model the electronic structure of the reactant, which has a *cis*-a_3b_2 ligand arrangement, and the acid–base complex product having a *fac*-a_3b_2c arrangement. Nuclear quadrupole resonance techniques offer a route to some of this information.

Second, experience has shown that NQR spectra are not routinely observed. Some compounds produce signals, while others do not. Although not explicitly recognized as such, NQR data have been obtained by superregenerative methods on a number of transition-metal complexes formally possessing the *fac*-a_3b_2c coordination sphere.[3-8] The variety of studies involving this geometry exceeds any other at the moment. It is premature to speculate on whether there are unique reasons why signals have readily appeared for metals in this coordinate geometry, but the pattern is worthy of note. At first sight the low symmetry of the *fac*-a_3b_2c coordination sphere might present a formidable interpretative task. However, by using an electrostatic model, qualitative information can be extracted with little difficulty.

Described herein is an interpretation of the nuclear quadrupole resonance spectra of Co(I) and Co(III) in several *fac*-a_3b_2c structures. Co(III) compounds of the type $CpCoI_2c$, where c is a 2e donor ligand, are the central focus of this investigation. These Co(III) complexes are compared to Mn(I) complexes to correlate the d-electron distribution between isoelectronic first-row transition elements. The Co(I) compounds are Lewis acid–base adducts in which the Co(I) atom is the Lewis base. The alterations in the electron density occurring when the free base engages in complex formation will be described elsewhere.

Results and Discussion

^{59}Co NQR Spectroscopy. ^{59}Co is an $I = {}^7/_2$ nucleus and yields a maximum of three spin-allowed transitions per unique nucleus. These transitions occur between $m_I^2 = \pm{}^7/_2 \leftrightarrow \pm{}^5/_2$ (ν_3), $\pm{}^5/_2 \leftrightarrow {}^3/_2$ (ν_2), and $\pm{}^3/_2 \tau \pm{}^1/_2$ (ν_1). In practice, ν_1 is much less intense than ν_2 or ν_3 and is detectable only when ν_2 and ν_3 are quite intense. Even without ν_1 the ^{59}Co nuclear quadrupole coupling constant, e^2Qq/h, and the asymmetry parameter, η, can be determined uniquely. Q is the nuclear quadrupole moment and q is the largest component of the electric field gradient tensor (**EFG**), which by convention is the zz component. A computer program was used to solve the eigenvalue equations for $I = {}^7/_2$ to extract e^2Qq/h and η from the frequency data.[9] The value of the coupling constant is directly proportional to the magnitude of the **EFG** detected by the nucleus. Hence, e^2Qq/h and the **EFG** are interchangeable when discussing trends in the NQR data. The asymmetry parameter measures the difference between the other two principal axis components of the **EFG**, i.e. $(q_{xx} - q_{yy})/q_{zz}$.

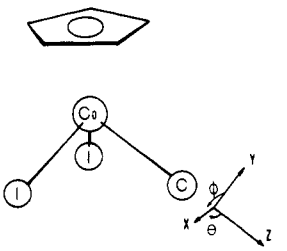

Figure 1. Structure of $CpCoI_2c$ complexes and the orientation of the principal axes of the electric field gradient at cobalt.

The *fac*-a_3b_2c Coordination Sphere. NQR studies have been conducted on a variety of organometallic complexes in which the metal atom lies at the center of a *fac*-a_3b_2c octahedral arrangement of ligands.[3-8] Well-defined examples involve Co(I) in $Co_3(CO)_9CR$[3] and Mn(I) in $CpMn(CO)_2c$.[4,5] In the former, one face of the octahedron of any Co atom is occupied by three CO groups. Two Co atoms are the b ligands and a C–R group is the unique ligand c. In the latter, η^5-$C_5H_5^-$ satisfies three valency positions on a face of the octahedron. The two carbonyl molecules and a group 5A based donor ligand are the b and c ligands, respectively.

Several other types of compounds formally possessing six electron pairs about the metal atom have been investigated. Although the coordination sphere is highly distorted, $Co_2(CO)_8$ and three terminal CO groups, two bridging CO's, and a metal–metal bond for each cobalt atom.[6] Similarly, $Co_2(CO)_6C_2R_2$ has three CO's, two olefin carbons, and a metal–metal bond about each cobalt atom.[7] The coordination sphere of Mn(I) in $C_6H_7Mn(CO)_3$ might be classed as a highly distorted octahedron.[8] The dienide portion of the C_6H_7 ligand is not entirely delocalized but the symmetry requires equivalency of two of the three electron pairs. Thus, if this face of the octahedron is the b_2c porition of the coordination sphere, the geometry is a highly distorted *fac*-a_3b_2c structure. Because of the large deviation from ideal octahedral geometry in terms of both the ligands and the electron density, high asymmetry of the electric field gradient is expected. The asymmetry parameters are indeed quite large.[6-8]

None of the compounds mentioned above constitutes a critical test of an electric field gradient model for *fac*-a_3b_2c octahedral structure. Therefore, another series of complexes was sought which better approximates an octahedral structure and permits ligand variations. The $CpCoI_2c$ system (Figure 1) is well-suited to these goals. The angles in the CoI_2c portion of the complex are approximately 90° by analogy to similar iron complexes,[10] and, in addition to a variety of ligands, c, complexes of the type $[\eta^5\text{-}C_5H_5CoIc_2]^+X^-$ may be prepared. The NQR data for these compounds are compiled in Table I. It should be noted that NQR spectra were observed in most of the compounds studied which further supports the hypothesis that factors may be optimal for obtaining signals in the *fac*-a_3b_2c coordinate geometry.

The *fac*-a_3b_2c Electric Field Gradient Model. Broadly applicable empirical electric field gradient models are necessarily qualitative in nature. In the spirit of crystal field theory of transition-metal ions[11] and partial field gradient models in Mössbauer spectroscopy,[12] a point-charge electrostatic description of the ligand's contribution to the electric field

(2) Werner, H.; Neukomm, H.; Klaui, W. *Helv. Chim. Acta* **1977**, *60*, 326–333.
(3) Miller, D. C.; Brill, T. B. *Inorg. Chem.* **1978**, *17*, 240–244.
(4) Anderson, W. P.; Brill, T. B.; Schoenberg, A. R.; Stanger, C. W. *J. Organomet. Chem.* **1972**, *44*, 161–169.
(5) Bryukhova, E. V.; Ginsberg, A. G.; Khotsyanova, T. L.; Saatsasov, V. V.; Semin, G. K. *Izv. Akad. Nauk SSSR, Ser. Khim.* **1973**, 661–663.
(6) Mooberry, E. S.; Spiess, H. W.; Garrett, B. B.; Sheline, R. K. *J. Chem. Phys.* **1969**, *51*, 1970–74.
(7) Chia, L. S.; Cullen, W. R.; Gerry, M. C. L.; Lerner, E. C. *Inorg. Chem.* **1975**, *14*, 2975–2980.
(8) Brill, T. B.; Fultz, W. C.; Hoffman, B. R. *Inorg. Chem.* **1980**, *19*, 749–751.
(9) Brill, T. B.; Hamilton, L. F., unpublished results.
(10) Miller, J. R.; Stephens, F. S. *J. Chem. Soc., Dalton Trans.* **1975**, 833–38.
(11) Bethe, H. *Ann. Phys. (Leipzig)* **1929**, *3*, 135–208.
(12) Parrish, R. V. *Prog. Inorg. Chem.* **1972**, *15*, 101–230. Bancroft, G. M.; Platt, R. H. *Adv. Inorg. Chem. Radiochem.* **1972**, *15*, 59–258.

Table I. ^{59}Co Nuclear Quadrupole Resonance Data in $(\eta^5\text{-}C_5H_5)CoI_2c$ and $[(\eta^5\text{-}C_5H_5)CoIc_2]^+I^-$ Complexes at 298 K

	frequencies, MHz[a]				
c	ν_3	ν_2	ν_1	e^2Qq/h, MHz	η
CO	26.528 (8)	17.682 (6)	8.850 (3)	123.80	0.020
$PO_3C_6H_{11}$[b]	27.075 (3)	17.830 (3)		126.72	0.171
$P(OC_6H_5)_3$[c]	27.512 (2)	18.220 (2)		128.58	0.122
	27.926 (3)	18.525 (3)		130.47	0.105
$P(C_6H_5)_3$	28.717 (4)	18.992 (4)		134.26	0.135
$Sb(C_6H_5)_3$	28.884 (7)	19.041 (7)		135.15	0.163
$As(C_6H_5)_3$	29.760 (5)	19.785 (6)		138.97	0.078
NC_5H_5	31.650 (8)	21.100 (8)	10.550 (2)	147.70	0.000
$NC_5H_5[4\text{-}C(CH_3)_3]$[c]	31.517 (5)	21.007 (3)		147.09	0.021
	31.936 (5)	21.275 (7)		149.06	0.039
$NH_2CH_2C_6H_5$	32.459 (20)	21.610 (20)	10.939 (2)	151.52	0.054
	frequencies, MHz[a]				
c_2	ν_3	ν_2	ν_1	e^2Qq/h, MHz	η
en[d]	32.371 (2)	21.559 (2)		151.10	0.047
phen[e]	32.683 (2)	21.787 (2)		152.52	0.012
bpy[f]	32.820 (25)	21.877 (20)	10.960 (3)	153.17	0.021

[a] Signal-to-noise ratios are given parenthetically. [b] Ethyl-3,5,8-trioxa-4-phosphabicyclo(2.2.2)octane. [c] Multiple resonances result from crystallographically inequivalent cobalt atoms. [d] Ethylenediamine. [e] *o*-Phenylenediamine. [f] Bipyridyl.

gradient was adopted here. Explanation of trends in the **EFG** rather than calculation of the **EFG** was sought, and so parameterization with bond distances and numerical partial **EFG** values of the ligands is unnecessary. By eliminating these variables the pure truth is lost, but a descriptive tool is gained. The justification for empirical approaches rests in their simplicity and utility. The electrostatic model has been used successfully before to interpret intramolecular **EFG** observations in metal complexes.[13,14]

The angular contribution of each ligand to the total **EFG** in the *fac*-a_3b_2c geometry can be computed by summing the contribution from each ligand to the individual elements of the tensor in eq 1. Octahedral geometry is assumed.

$$q = \begin{bmatrix} 3e(\sin^2\theta\cos^2\phi - 1) & 3e(\sin^2\theta\sin\phi\cos\phi) & 3e(\sin\theta\cos\theta\cos\phi) \\ 3e(\sin^2\theta\sin\phi\cos\phi) & 3e(\sin^2\theta\sin^2\phi - 1) & 3e(\sin\theta\cos\theta\sin\phi) \\ 3e(\sin\theta\cos\theta\cos\phi) & 3e(\sin\theta\cos\theta\sin\phi) & 3c(\cos^2\theta - 1) \end{bmatrix} \quad (1)$$

The Z axis of the **EFG** is chosen to coincide with the bond between the cobalt atom and the unique ligand, c, as shown in Figure 1. Other orientations might be chosen, but as noted below none is consistent with the experimental data in Table I. This orientation has been selected in several previous investigations.[3,7,8] When the Z axis is oriented in this manner, the largest principal axis component of the **EFG** tensor, q_{zz}, at the metal atom depends only on the **EFG** contributions of ligands b and c according to eq 2.[15] The asymmetry parameter, η, at the metal is calculated to be 0 despite the low symmetry of the coordination sphere. Thus, if b is held constant, c is varied, and octahedral geometry is maintained, the NQR coupling constant will vary in concert with known bonding properties of c. The asymmetry parameter should remain small or be 0. If the coordination sphere becomes *fac*-a_3b_2c, the point-charge model predicts that the sign, but not the magnitude, of q_{zz} will change. Of course, the sign of the **EFG** cannot be extracted from pure NQR spectra, and so the same coupling constant and asymmetry parameter should be observed in *fac*-a_3b_2c and *fac*-a_3bc_2 complexes.

$$q_{zz} = 2q_{zz}^{b} - 2q_{zz}^{c} \quad (2)$$

Application of the Coordination Sphere Model to Co(III) and Mn(I) NQR Data. A test of this coordination sphere approach in the *fac*-a_3b_2c geometry lies in the data for $CpCoI_2c$ and $[CpCoIc_2]^+$ complexes given in Table I. In the former the range of ligands c covers strong π-acceptor/weak σ-donor ligands (carbonyl) to weak π-acceptor/strong σ-donor ligands (amines). The trend in the ^{59}Co coupling constants exhibits a clear progression. The **EFG** at the cobalt atom is highest when c = amine. As the σ-donor ability of c decreases and its π-acceptor ability increases through the series from amines to the phosphines, to the phosphites, and finally to CO, the **EFG** steadily decreases. This trend results from the fact that the iodine atoms (the b ligands) remain constant, while c changes. q_{zz} in eq 2 therefore depends on the bonding properties of c alone. The values of η vary erratically from 0.00 to 0.17 but are small owing to the approximately octahedral geometry of the complexes. The nonzero values probably arise from distortions brought on by crystal-packing forces because no correlation exists between η and the bonding properties or steric demands of c. Hence the coordination sphere approach to the **EFG** allows one to rationalize the NQR results for $CpCoI_2c$ complexes. It was useful for predicting the shifts of the ^{59}Co signals produced by the ligands during this study.

The coordination sphere model predicts the same ^{59}Co NQR parameters for $CpCoI_2c$ and $CpCoIc_2^+$ with a given ligand, c. Table I contains data for the bidentate nitrogen donor ligands ethylenediamine, *o*-phenylenediamine, and bipyridyl, which are c_2 ligands that form salts having the stoichiometry, $[CpCoIc_2]^+I^-$. These complexes yield NQR data which are very similar to those produced by $CpCoI_2c$, where c = pyridine and benzylamine. This observation concurs with the prediction of the point-charge model given in the preceding section.

While the formalism described above accounts for the NQR data in $CpCoI_2c$ complexes, the scope of the approach can be established by including other classes of compounds. The model predicts that the **EFG** at the cobalt atoms in $Co_3(CO)_9CR$ should directly relate to the electronic character of R as R is varied. Indeed, the ^{59}Co coupling constants vary in unison with the resonance parameter, σ_R^-, of R.[3] The values of η lie in the range of 0.18–0.28 due to the distorted octahedral coordination sphere about the cobalt atoms, but no correlation exists between η and properties of R. Hence, the predictions of the model bear up well to all of the experimental

(13) Brown, T. L.; LaRossa, R. A. *J. Am. Chem. Soc.* **1974**, *96*, 2072–2081. Brown, T. L. *Acc. Chem. Res.* **1974**, *7*, 408–415.
(14) Brill, T. B. *J. Magn. Reson.* **1974**, *15*, 395–401.
(15) The contribution of the Cp ring (=A_3) to the EFG is substantial according to the EFG apparently generated by two Cp rings in Cp_2Co^+ salts (Brill, T. B. *Adv. Nucl. Quadrupole Reson.* **1978**, *3*, 131–183 and references therein). However, the EFG from Cp is a constant factor.

Table II. ^{59}Co Nuclear Quadrupole Resonance Data in Other Co(III) and Co(I) Complexes Having the *fac*-a_3b_2c Ligand Geometry (298 K)

complex	frequency, MHz[a] ν_3	ν_2	e^2Qq/h, MHz	η
$CpCo(CO)_2HgCl_2$[b]	23.157 (7)	15.117 (7)	108.66	0.233
$CpCo(CO)_2HgBr_2$	23.538 (8)	15.243 (5)	110.77	0.287
$CpCo[P(O)(OCH_3)_2]_2[P(OCH_3)_3]$	22.482 (11)	14.590 (5)	105.71	0.272

[a] Parenthetical numbers are signal-to-noise ratios. [b] $\nu(^{35}Cl)$ = 18.844 (5) MHz.

findings for $Co_3(CO)_9CR$ complexes.

In $CpMn(CO)_2c$ complexes, a recognizable correlation is found between the $\pm^3/_2 \leftrightarrow \pm^5/_2$ transition of ^{55}Mn and the σ/π-bonding characteristics of the Lewis base ligands, c, drawn from the group 5A elements.[4] Strong σ donors appear at one end while strong π acceptors appear at the other. A correlation of this type is expected from eq 2. The highest frequency transition rather than the coupling constant was used in this correlation because the $\pm^1/_2 \leftrightarrow \pm^3/_2$ transition was often too weak to detect. The $\pm^3/_2 \leftrightarrow \pm^5/_2$ transition frequency mimics the coupling constant provided η is relatively constant. This assumption is reasonable based on the few available values of η for these compounds.[5] The correlation between the bonding properties of c and the ^{55}Mn NQR frequency in these $CpMn(CO)_2c$ complexes further supports the coordination sphere approach, but the nonnegligible values of η require further comment.

The few available values of η in $CpMn(CO)_2c$ complexes, where c is a single atom donor, lie in the range of 0.19–0.27.[5] These values may typify two carbonyl groups in the *fac*-a_3b_2c coordination sphere. For instance, values of η in the neighborhood of 0.26 are observed for $CpCo(CO)_2c$, where c = $HgCl_2$ and $HgBr_2$ (Table II). In these latter compounds, the transition-metal site is a Lewis base and c is a Lewis acid. The cobalt atom is formally Co(I). Thus, while the amount of data is small, it is evident that two carbonyl groups as the b ligands in the *fac*-a_3b_2c geometry produce values of η in the range of 0.20–0.30. Such asymmetry might be related to the asymmetry in metal–CO π back-bonding,[16] although the picture is not yet clear. When π-olefin ligands are present in the coordination sphere either as the unique ligand, c, or as the b ligands, large values of η are observed,[4,7,8] and the point-charge model does not describe the **EFG**. The substantial asymmetry no doubt results from redistribution of metal d-electron density which occurs when a π olefin replaces a simple Lewis base ligand in the coordination sphere.

The assessment of the electric field gradient generated by weak σ-donor/strong π-acceptor ligands aids in characterizing the bonding of an uncommon ligand, the phosphonate group, to Co(III). Recently, $CpCo[P(O)(OCH_3)_2]_2[P(OCH_3)_3]$ was synthesized by a double Michaelis–Arbusov reaction between $P(OCH_3)_3$ and $CpCoI_2(CO)$.[17] Its molecular structure was determined by X-ray crystallography.[17] The geometry about the Co(III) atom is *fac*-a_3b_2c. e^2Qq/h and η for the complex (Table II) are close to the values for $CpCo(CO)_2HgX_2$ (X = Cl, Br). We conclude that the phosphonate group is a relatively weak σ-donor ligand with some π-acceptor capability. Because the σ bond largely controls the bond distance, the Co–P bond distances in $CpCo[P(O)(OCH_3)_2]_2[P(OCH_3)_3]$ should reflect the low σ-donor ability of the phosphonate ligand. The cobalt–phosphonate bonds are significantly longer than the cobalt–phosphite bond,[17] indicating that the Co(II-I)–P(V) bond is weaker than the Co(III)–P(III) bond. This bonding description of the phosphonate group reaffirms the point that weak σ-donor/strong π-acceptor ligands at the b sites generate nonnegligible values of η in the *fac*-a_3b_2c geometry.

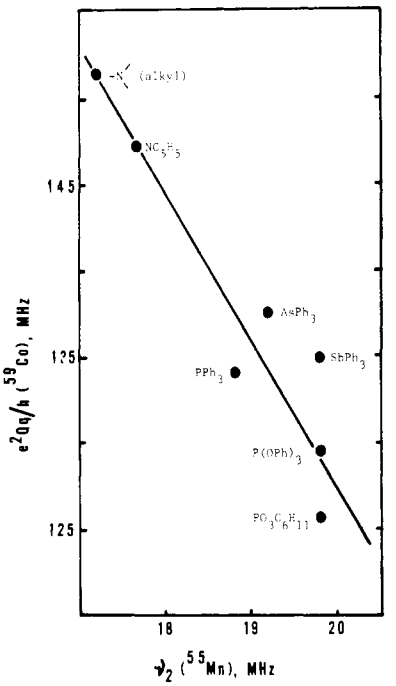

Figure 2. Correlation between the electric field gradient at isoelectronic Co(III) and Mn(I) sites in $CpCoI_2c$ and $CpMn(CO)_2c$ where the ligand, c, is common to both.

In summary, the point-charge coordination sphere model for *fac*-a_3b_2c structures works well when the geometry approaches octahedral and the b and c ligands engage in predominantly 2e single bonds. The model is less satisfactory but is still qualitatively representative when the b ligands have single atom donor sites but display considerable π acidity. Not surprisingly, the model fails to describe the NQR data when the b or c ligands are π olefins. The bonding contributions of such ligands are too complex to conform to an electrostatic model.

Correlations of Co(III) and Mn(I) NQR Data. Further details about the electron distribution of the Co(III) organometallics in Table I are gained by using the approximation that the populations, N, of the Co 3d orbitals are the transmitting factor in the electric field gradient, q_{zz}. This approximation leads to eq 3. The small values of η in the

$$(e^2Qq_{zz}/h)_{\text{molecule}} = (e^2Qq_{zz}/h)_{\text{atom}}\left[N_{d_{z^2}} + \frac{N_{d_{xz}} + N_{d_{yz}}}{2} - N_{d_{xy}} - N_{d_{x^2-y^2}}\right] \quad (3)$$

$CpCoI_2c$ complexes are consistent with location of the Z axis of the **EFG** tensor along the Co–C bond. The Z axis coincides with d_{z^2} orbital when eq 3 is used. Strong σ-donor ligands at the site c increase the population of the d_{z^2} orbital while strong π acidity of c reduces the population of the d_{xz} and d_{yz} orbitals. Therefore, σ and π bonding are opposed forces in controlling the magnitude of the positive terms in eq 3. In accordance with this prediction, the lowest coupling constants in Table I are produced by weak σ-donor/strong π-acceptor ligands (CO and $PO_3C_6H_{11}$), while the largest values result from strong σ-donor/weak π-acceptor ligands such as the amines. This ordering requires the numerical sum of the positive terms in eq 3 to exceed that of the negative terms.

(16) (a) Kettle, S. F. A. *Inorg. Chem.* **1965**, *4*, 1661–1663. (b) Kettle, S. F. A. *J. Chem. Soc.* **1966**, 420–422.
(17) Towle, D. K.; Landon, S. J.; Brill, T. B.; Tulip, T. H. *Organometallics* **1982**, *1*, 295–301.

The d-electron distribution in $CpCoI_2c$ complexes of Co(III) can be compared to that in complexes of isoelectronic Mn(I), $CpMn(CO)_2c$, where c is the same ligand.[4] A plot of the $\pm^3/_2 \leftrightarrow \pm^5/_2$ transition of ^{55}Mn vs. the ^{59}Co coupling constant is shown in Figure 2. The reason for using the $\pm^3/_2 \leftrightarrow \pm^5/_2$ transition of ^{55}Mn in this comparison was noted above. The correlation between the cobalt and manganese data indicates that the common ligand c has the opposite effect on the two complexes. Strong σ-donor/weak π-acceptor ligands generate the highest **EFG** in $CpCoI_2c$ but the lowest **EFG** in $CpMn(CO)_2c$. The reverse is witnessed for weak σ-donor/strong π-acceptor ligands. This inversion is caused by differences in the d-electron distribution which gives the **EFG** the opposite sign for these two metals. It was noted above that the positive terms of eq 3 outweigh the negative terms for the Co(III) complexes. Because the reverse **EFG** trend is observed for the Mn(I) complexes, the magnitude of the negative terms in Mn(I) must outweigh the positive terms.

The sign difference of the **EFG** between Co(III) and Mn(I) probably results from differences in the b ligands of the *fac*-a_3b_2c structure. CO is a weaker σ donor than I^-. As a result, the $d_{x^2-y^2}$ and/or d_{xy} orbitals of Mn(I) are less populated than those of Co(III) in these complexes. Furthermore, the loss of electron density from the d_{xz} and d_{yz} orbitals of Mn(I) due to Mn(I)→CO π back-bonding, which does not occur in the Co^{III}–I bond, diminishes the magnitude of the positive terms in eq 3. The d_{xz} and d_{yz} orbitals of Co(III) in fact may gain a small amount of electron density from Co←I π bonding. These effects work toward increasing the magnitude of the positive terms in Co(III) while decreasing them in Mn(I). The extent to which this occurs is large enough to reverse the sign of the **EFG**.

The above comparison between Co(III) and Mn(I) helps reconcile conflicting discussions that have arisen regarding the Mn(I) complexes.[4,18,19] From a Mössbauer study of several $CpFe(CO)_2c^+$ salts,[19] it was concluded that the sign of the bracketed quantity in eq 3 was chosen incorrectly in previous work on Mn(I) and that it must have a negative value. By inference, the sign in $CpMn(CO)_3$ was also proposed to be negative,[19] but this choice conflicts with a large body of data.[5,18,20] The present study demonstrates that the sign of the bracketed quantity is indeed negative for $CpMn(CO)_2c$ and therefore is opposite that found for $CpMn(CO)_3$. The confusion in these systems is caused by a heretofore unrecognized reorientation of the *Z* **EFG** axis of the metal atom which occurs on going from $CpMn(CO)_3$ to $CpMn(CO)_2c$. In the case of $CpMn(CO)_3$, symmetry requires that the *Z* axis coincide with a line passing through the metal atom and the center of the cyclopentadienyl ring. The bracketed quantity of eq 3 is clearly positive in $CpMn(CO)_3$.[5,18,20] On the other hand, the *Z* axis in $CpMn(CO)_2c$ is located along the metal–c bond. The iron Mössbauer data[19] point toward a negative sign for thee bracketed quantiy. Consequently, the *Z* axis rotates through approximately a tetrahedral angle and changes sign on going from $CpMn(CO)_3$ to $CpMn(CO)_2c$.

In conclusion, an electrostatic model of the **EFG** at the transition metal in a *fac*-a_3b_2c ligand coordination sphere successfully explains experimental NQR spectra. The approach works best when the b and c ligands are not strong π acids. This formalism gives a basis for discussing electronic differences in isoelectronic complexes and will be employed in future studies dealing with electronic rearrangements that occur at the metal during organometallic and acid/base reactions.

Experimental Section

Syntheses. All solvents were reagent grade or better and used as received. $CpCo(CO)_2$ (Strem), $(C_5H_5)_3Sb$ (ROC/RIC), and $(C_6H_5O)_3P$ (ROC/RIC) were used without further purification. $CpCoI_2(CO)$, $CpCoI_2[P(C_6H_5)_3]$, $CpCoI_2(NH_2CH_2C_6H_5)$, $CpCoI_2(PO_3C_6H_{11})$, [CpCoI(bpy)]I, and [CpCoI(en)]I were prepared by the methods of Heck[21] and King.[22] $CpCoI_2[As(C_6H_5)_3]$,[23] [CpCoI(phen)]I,[24] $CpCo(CO)_2HgCl_2$,[1] $CpCo(CO)_2HgBr_2$,[1] and $CpCo[P(O)(OCH_3)_2]_2[P(OCH_3)_3]$[17] were prepared by published procedures.

^1H NMR spectra were obtained by using either a Perkin-Elmer R-12B or a Bruker WM-250 spectrometer and are reported relative to $(Me)_4Si$ ($\delta = 0.00$). $^{13}C\{^1H\}$ and $^{31}P\{^1H\}$ spectra were recorded on a Bruker WM-250 and are reported relative to $(Me)_4Si$ and external H_3PO_4, respectively. Melting points were measured in open capillary tubes with a Melt-Temp heating block and are uncorrected.

Synthesis of $(\eta^5\text{-}C_5H_5)CoI_2[Sb(C_6H_5)_3]$. A solution of 2.102 g (5.18 mmol) of $CpCoI_2(CO)$ in 100 mL of CH_2Cl_2 was slowly added to 2.232 g (6.32 mmol) of $(C_6H_5)_3Sb$ in 100 mL of CH_2Cl_2 with vigorous stirring. The solution, initially dark blue, turned emerald green after several minutes. Stirring was continued for 1 h. The mixture was filtered and the volume reduced to 75 mL. The addition of an equal volume of hexane followed by slow removal of solvent produced dark green crystals. The crystals were washed with three 50-mL portions of hexane and allowed to air-dry, producing 3.24 g of product (87% yield based on $CpCoI_2(CO)$); mp 179–180 °C. $(\eta^5\text{-}C_5H_5)CoI_2[Sb(C_6H_5)_3]$ is soluble in most polar organic solvents. It decomposes slowly in air in a few months. ^1H NMR ($CDCl_3$): 7.726, 7.432 ppm (C_6H_5, 15 H), 5.202 ppm (Cp, 5 H). ^{13}C NMR ($CDCl_3$): 135.54, 132.19, 130.69, 129.19 ppm (C_6H_5), 83.17 ppm (Cp). Anal. Calcd for $C_{23}H_{20}CoI_2Sb$: C, 37.80; H, 2.73; Co, 8.16. Found: C, 37.65; H, 2.58; Co, 8.19.

Synthesis of $(\eta^5\text{-}C_5H_5)CoI_2[P(OC_6H_5)_3]$. To a solution of 1.902 g (6.13 mmol) of $(C_6H_5O)_3P$ in 175 mL of CH_2Cl_2 was added 2.802 g (6.13 mmol) of $[\eta^5\text{-}C_5H_5)CoI_2(NC_5H_5)]$ in 50 mL of CH_2Cl_2 with vigorous stirring. The solution changed from green to deep brown within a few minutes. The solution was allowed to stir for 1 h and the solvent removed under reduced pressure at 25 °C, leaving a purple-black solid. So that the odor of pyridine could be removed, the solid was dried overnight in a vacuum oven at 40 °C: mp 164–165 °C; 2.279 g (55% yield based on $[CpCoI_2(NC_5H_5)]$). The complex is soluble in polar organic solvents and insoluble in nonpolar solvents. ^1H NMR ($CDCl_3$): 7.55 ppm (m, 15 H), 5.26 ppm (d, 5 H, $J_{H-P} = 0.87$ Hz). ^{13}C NMR ($CDCl_3$): 151.5, 129.5, 124.1, 120.6 ppm (C_6H_5), 86.26 ppm (Cp). ^{31}P ($CDCl_3$): 129.07 ppm (br). Anal. Calcd for $C_{23}H_{20}CoI_2O_3P$: C, 40.15; H, 2.90; Co, 8.56; P, 4.49. Found: C, 39.92; H, 2.62; Co, 8.61; P, 4.53.

NQR Spectra. The NQR data were recorded on a Wilks NQR-1A superregenerative oscillator spectrometer at 298 K.[25] The sample quantities varied from 0.5 to 2.0 g. Due to the difficulty of measuring the center line of the resonance multiplet, the frequencies are accurate to 0.005 below 20 MHz and 0.008 above 20 MHz.

Registry No. $(\eta^5\text{-}C_5H_5)CoI_2(CO)$, 12012-77-0; $(\eta^5\text{-}C_5H_5)CoI_2(PO_3C_6H_4)$, 12153-44-5; $(\eta^5\text{-}C_5H_5)CoI_2(P(OC_6H_5)_3)$, 80642-49-5; $(\eta^5\text{-}C_5H_5)CoI_2(P(C_6H_5)_3)$, 12194-27-3; $(\eta^5\text{-}C_5H_5)CoI_2(Sb(C_6H_5)_3)$, 80642-50-8; $(\eta^5\text{-}C_5H_5)CoI_2(As(C_6H_5)_3)$, 80642-51-9; $(\eta^5\text{-}C_5H_5)CoI_2(NC_5H_5)$, 12146-14-4; $(\eta^5\text{-}C_5H_5)CoI_2(NH_2CH_2C_6H_5)$, 33198-58-2; $[(\eta^5\text{-}C_5H_5)CoI(en)]I$, 33291-98-4; $[(\eta^5\text{-}C_5H_5)CoI(phen)]I$, 12212-83-8; $[(\eta^5\text{-}C_5H_5)CoI(bpy)]I$, 12147-68-1; $CpCo(CO)_2HgCl_2$, 80642-52-0; $CpCo(CO)_2HgBr_2$, 80642-53-1; $CpCo[P(O)(OCH_3)_2]_2[P(OCH_3)_3]$, 79018-66-9.

(18) Brill, T. B.; Kotlar, A. J. *Inorg. Chem.* **1974**, *13*, 470–474.
(19) Bancroft, G. M.; Butler, K. D.; Manzer, L. E.; Shaver, A.; Ward, J. E. H. *Can. J. Chem.* **1974**, *52*, 782–87.
(20) Brill, T. B.; Long, G. G. *Inorg. Chem.* **1970**, *10*, 74–77.
(21) Heck, R. F. *Inorg. Chem.* **1965**, *4*, 855–857.
(22) King, R. B. *Inorg. Chem.* **1966**, *5*, 82–87.
(23) Yamazaki, H.; Hagihara, N. *J. Organomet. Chem.* **1970**, *21*, 431–443.
(24) Heck, R. F. *Inorg. Chem.* **1968**, *7*, 1513–1516.
(25) Brill, T. B.; Long, G. G. *J. Phys. Chem.* **1971**, *75*, 1898–1900.